

Viral Bcl-2 Encoded by the Kaposi's Sarcoma-Associated Herpesvirus Is Vital for Virus Reactivation

Anastasia Gelgor,^a Inna Kalt,^a Shir Bergson,^a Kevin F. Brulois,^b Jae U. Jung,^b and Ronit Sarid^a

The Mina and Everard Goodman Faculty of Life Sciences, Bar Ilan University, Ramat-Gan, Israel^a; Department of Molecular Microbiology and Immunology, Keck School of Medicine, University of Southern California, Los Angeles, California, USA^b

ABSTRACT

The Kaposi's sarcoma-associated herpesvirus (KSHV) open reading frame 16 (*orf16*) encodes a viral Bcl-2 (vBcl-2) protein which shares sequence and functional homology with the Bcl-2 family. Like its cellular homologs, vBcl-2 protects various cell types from apoptosis and can also negatively regulate autophagy. vBcl-2 is transcribed during lytic infection; however, its exact function has not been determined to date. By using bacterial artificial chromosome 16 (BAC16) clone carrying the full-length KSHV genome, we have generated recombinant KSHV mutants that fail to express vBcl-2 or express mCherry-tagged vBcl-2. We show that the vBcl-2 protein is expressed at relatively low levels during lytic induction and that a lack of vBcl-2 largely reduces the efficiency of KSHV reactivation in terms of lytic gene expression, viral DNA replication, and production of infectious particles. In contrast, the establishment of latency was not affected by the absence of vBcl-2. Our findings suggest an important role for vBcl-2 during initial phases of lytic reactivation and/or during subsequent viral propagation. Given the known functions of vBcl-2 in regulating apoptosis and autophagy, which involve its direct interaction with cellular proteins and thus require high levels of protein expression, it appears that vBcl-2 may have additional regulatory functions that do not depend on high levels of protein expression.

IMPORTANCE

The present study shows for the first time the expression of endogenous vBcl-2 protein in KSHV-infected cell lines and demonstrates the importance of vBcl-2 during the initial phases of lytic reactivation and/or during its subsequent propagation. It is suggested that vBcl-2 has additional regulatory functions beyond apoptosis and autophagy repression that do not depend on high levels of protein expression.

Kaposi's sarcoma-associated herpesvirus (KSHV), also referred to as human herpesvirus 8 (HHV-8), is a gamma-2 herpesvirus. KSHV is causally linked to particular human cancers, including Kaposi's sarcoma (KS), primary effusion lymphoma (PEL), and plasmablastic multicentric Castleman's disease (1–7). Among human viruses, KSHV is most closely related to the Epstein-Barr virus (EBV), a tumorigenic gamma-1 herpesvirus known to be associated with lymphomas and nasopharyngeal carcinoma. Like all other herpesviruses, the infectious cycle of KSHV includes two alternative infection phases, latent and lytic. Latent infection allows the virus to establish long-term persistent infection and involves the presence of viral episomes and expression of a small set of viral genes. Lytic infection is needed for the maintenance of viral reservoirs and for virus spread and involves a temporally regulated cascade of viral gene expression and DNA replication, leading to the production and release of new virions. KSHV exists mainly in its latent form in KS lesions and in PEL, yet a small subpopulation of cells undergoes lytic replication. Analogously, most KSHV-infected cultured cells are latently infected. Lytic virus reactivation can be induced in these cells by treatment with a variety of soluble cytokines, coinfection by another viral agent, or treatment with chemical reagents, such as 12-*O*-tetradecanoylphorbol-13-acetate (TPA) and sodium butyrate. Initiation of lytic replication proceeds mainly through the activities of the viral replication and transcription activator (RTA) protein, which activates the expression of certain KSHV genes, eventually leading to the upregulation of all the lytic cycle KSHV genes (8–12). Yet an alternative RTA-independent emergency replication program is

triggered by caspase-3 activation and provides the virus with a last chance of reproducing before the completion of host cell apoptosis (13).

The Bcl-2 family of proteins comprises vital mitochondrial permeability regulators of apoptosis that integrate diverse survival and death signals (14–17). Members of the Bcl-2 family are defined by the presence of up to four conserved Bcl-2 homology (BH) domains (BH1 to BH4), while several members also possess a carboxy-terminal transmembrane domain, which mediates their association with intracellular membranes. Bcl-2 homologues are encoded by all gammaherpesviruses and generally share 20 to 30% homology with one another and with their cellular counterparts (18). The conservation of Bcl-2 homologues in these viruses suggests their importance in evolutionarily conserved functions.

KSHV open reading frame 16 (*orf16*) encodes an antiapoptotic viral Bcl-2 (vBcl-2) protein which shares sequence and functional homology with members of the Bcl-2 family (19, 20). Like most

Received 13 January 2015 Accepted 26 February 2015

Accepted manuscript posted online 4 March 2015

Citation Gelgor A, Kalt I, Bergson S, Brulois KF, Jung JU, Sarid R. 2015. Viral Bcl-2 encoded by the Kaposi's sarcoma-associated herpesvirus is vital for virus reactivation. *J Virol* 89:5298–5307. doi:10.1128/JVI.00098-15.

Editor: R. M. Longnecker

Address correspondence to Ronit Sarid, saridr@mail.biu.ac.il.

Copyright © 2015, American Society for Microbiology. All Rights Reserved.

doi:10.1128/JVI.00098-15

herpesvirus homologues of Bcl-2, vBcl-2 demonstrates conserved sequences in both the BH1 and BH2 domains, but it has only a low degree of homology with other regions of Bcl-2. Still, vBcl-2 shares 3-dimensional structural conservation with other Bcl-2 family members and includes the conserved BH3 binding groove and a hydrophobic membrane anchor domain. The BH3 binding cleft of vBcl-2 binds to peptides encoding BH3 domains present on the proapoptotic proteins Noxa, Bik, PUMA, Bak, Bax, Bid, Bim, and Bad (21–23). vBcl-2 also forms a stable complex with the cellular protein Aven, which binds Apaf-1 and is known to be a regulator of caspase-9 and ataxia telangiectasia (ATM) activation (24, 25). However, unlike the cellular Bcl-2, vBcl-2 is not a substrate for KSHV–cyclin–cyclin-dependent kinase 6 (CDK6) phosphorylation (26) and cannot be converted to a proapoptotic molecule via caspase cleavage (27). Like the cellular and other virally encoded Bcl-2 proteins, vBcl-2 binds Beclin-1 (28, 29). The association between vBcl-2 and the Beclin-1–phosphoinositol 3-kinase C3 (PI3KC3)–UVRAG autophagic complex mediates negative regulation of autophagy, which, unlike the case of cellular Bcl-2, is not disrupted by Jun N-terminal protein kinase 1 (JNK1) phosphorylation (28, 30, 31).

The function of vBcl-2 during virus infection has not been determined to date. vBcl-2 is transcribed during lytic virus infection (20, 32, 33). Thus, inhibition of apoptosis and autophagy by vBcl-2 may provide an attractive mechanism for prolonging the life span of KSHV-infected cells, which in turn enables increased virus production, establishment of latency, and/or efficient reactivation. Of note, transcripts encoding vBcl-2 were detected during lytic infection in various KSHV-infected cell cultures, yet the expression of vBcl-2 protein has been detected only in Kaposi's sarcoma lesions (34). Whether the function of vBcl-2 is necessary for KSHV-mediated oncogenesis is still unknown.

In an effort to increase our understanding of the function of vBcl-2 in the context of viral infection, we constructed mCherry-tagged and vBcl-2-null recombinant viruses. Using a bacterial artificial chromosome (BAC) 16 (BAC16) clone carrying the full-length KSHV genome, we generated KSHV genomes that fail to express vBcl-2 and a clone which expresses mCherry-tagged vBcl-2. We show that the vBcl-2 protein is expressed at low levels during lytic induction and that a lack of vBcl-2 largely reduces the efficiency of KSHV reactivation in terms of lytic gene expression, viral DNA replication, and production of infectious particles.

MATERIALS AND METHODS

Cells. HEK-293T, SLK, and iSLK cells (kindly provided by Don Ganem and Rolf Renne) (35) were maintained in Dulbecco's modified Eagle's medium (DMEM) supplemented with 10% fetal bovine serum (FBS) or Tet system-approved certified FBS (Biological Industries, Kibbutz Beit Haemek, Israel), 50 IU/ml penicillin, and 50 µg/ml streptomycin (Biological Industries, Kibbutz Beit Haemek, Israel). Two hundred fifty micrograms per milliliter of G418 and 1 µg/ml of puromycin (A. G. Scientific Incorporated) were added to the iSLK cell growth medium to maintain the Tet-On transactivator and RTA expression cassette, respectively.

Construction of BAC16-vBcl-2-stop, BAC16-mCherry-vBcl-2, and BAC16-mCherry-vBcl-2-stop recombinant viruses. BAC16 containing a recombinant full-length KSHV genome with a green fluorescent protein (GFP) cassette under the control of the elongation factor 1α (EF-1α) promoter has been previously described (36). The construction of the recombinant viruses was accomplished using *Escherichia coli* GS1783, whose genome encodes inducible bacteriophage lambda Red and I-SceI activities, with a two-step recombination protocol, as described previ-

ously (37). To construct a recombinant KSHV BAC16 clone containing a stop codon within *orf16* (BAC16-vBcl-2-stop), a recombination fragment was first generated by PCR using plasmid pEGFP-N1 (Clontech) carrying a kanamycin resistance (Kan^r) cassette as the template and primers flanking the desired stop codon of *orf16*. The primer set used to amplify this fragment was 5'-ACGAGGACGTTTTGCCTGGAGAGGTGTTGGCCA TTGAAGGGATATTCTAGGCCTGTGGATTAACGAACCTtagggataac agggtaatAGGTGGCACTTTTCGGGAAA-3' (the first 71 nucleotides [nt] complement *orf16* nt 5 to 76 and correspond to nt 29965 to 30036 of BAC16, while the stop codon is in boldface, the I-SceI restriction site is in lowercase letters, and the kanamycin resistance gene sequence is underlined) and 5'-GGGCTGAGCAAAGGATGGTACAGGTAAGGTTTC GTTTAATCCACAGGCCTAGAATATCCCTTCAATGGTTTATTGCC GTCATAGCGCGG-3' (the first 70 nt complement *orf16* nt 104 to 35 and correspond to nt 30065 to 29995 of BAC16, while the stop codon is shown in boldface and the kanamycin resistance gene sequence is underlined). Integration of the Kan^r/I-SceI cassette was verified by PCR, and that was followed by restriction enzyme digestion of the purified BAC16 DNA. Primers for sequences located upstream of *orf16* (nt 29941 to 29960; 5'-T GCCCTGGTGACCGTCCACA-3') and within the *orf16* coding sequence (nt 30423 to 30408; 5'-TGTCATTCTCCGTCC-3') were used to amplify a diagnostic DNA fragment of 482 bp, whereas a DNA fragment of 2,041 bp was obtained, as predicted, after insertion of the Kan^r/I-SceI cassette. The integrated cassette was then cleaved upon treatment with 1% L-arabinose; a second recombination event between the duplicated sequences resulted in the loss of the Kan^r/I-SceI cassette and recircularization of the BAC16 DNA, yielding kanamycin-sensitive colonies that were screened by replica plating, followed by diagnostic PCR as well as restriction enzyme digestion of the purified DNA. BAC DNA was purified using a large-construct kit (Qiagen) according to the manufacturer's instructions. BAC DNA was digested with BamHI and run on a 0.4% agarose gel. The inserted DNA fragment was sequenced to confirm the stop mutation. To construct a virus expressing the mCherry protein fused to the 5' end of vBcl-2 (BAC16-mCherry-vBcl-2) and the mCherry protein inserted into BAC16-vBcl-2-stop (BAC16-mCherry-vBcl-2-stop), we employed the universal transfer plasmid pEP-mCherry (38). This plasmid was used as a PCR template to obtain a linear DNA fragment encompassing the kanamycin resistance cassette and an I-SceI restriction site, flanked by mCherry containing a small internal duplication, and flanking 47 bp of viral sequences from nucleotides 29914 to 29961 and 30011 to 29965, located upstream and downstream of the KSHV *orf16* start codon, respectively. The primer set used to amplify this fragment was 5'-CACCCCTG GTGCTGTGCGCGTGCTATGTGCCCTGGTGACCGTCCACAATG GTGAGCAAGGGCGAGGAGGATAAC-3' and 5'-AATATCCCTTCA ATGGCCAACACCTCTCCAGGCAAAACGTCCTCGTCCCTGTGACA GCTCGTCCATGC-3' (the mCherry start methionine codon is in boldface; the sequence homologous to that of mCherry is underlined). The purified PCR product of 1,786 bp was subsequently introduced into the GS1783 *E. coli* strain harboring BAC16 or BAC16-vBcl-2-stop. Integration of the mCherry/Kan^r/I-SceI cassette was verified by PCR to yield a 2,268-bp product as an indication for insertion and restriction enzyme digestion, as described above. A second recombination event was also followed by diagnostic PCR, restriction enzyme digestion, and sequencing of the purified DNA.

Transfection of KSHV BAC16 DNA and virus reconstitution. For BAC16 transfection and reconstitution, HEK-293T cells were grown to ~70% confluence in a 24-well plate, followed by transfection with 500 ng of BAC DNA via the Lipofectamine 2000 transfection reagent (Life Technologies, Invitrogen). Infected cells were selected in a medium that also contained 200 µg/ml hygromycin B (A. G. Scientific Incorporated). Following selection of HEK-293T cells carrying recombinant viruses, these cells were subcultured and mixed at a 1:1 ratio with iSLK cells. After 24 h, a lytic virus cycle was induced by 20 ng/ml 12-*O*-tetradecanoylphorbol-13-acetate (TPA) and 1 mM sodium butyrate (Sigma). Selection medium

containing 250 $\mu\text{g/ml}$ G418, 1 $\mu\text{g/ml}$ puromycin, and 1.2 mg/ml hygromycin B was added 4 days later, and iSLK cells infected with the recombinant viruses were established. KSHV-infected iSLK cells were treated with 1 $\mu\text{g/ml}$ doxycycline and 1 mM sodium butyrate (Sigma), in the absence of hygromycin, puromycin, and G418, to induce RTA transgene expression and lytic cycle reactivation. To purify virions, 4 days after lytic induction, supernatant was collected and cleared of cells and debris by centrifugation ($700 \times g$ for 10 min at 4°C) and filtration (0.45- μm -pore-size cellulose acetate filters; Corning). Virus particles were pelleted by centrifugation ($40,000 \times g$ for 2 h at 4°C).

Real-time reverse transcription-PCR. Total RNA was extracted by use of an EZ-RNA total RNA isolation kit (Biological Industries, Israel). Residual DNA contamination was eliminated by subsequent treatment with DNase by using a Turbo DNA-free kit (Ambion). cDNA was generated from 1 μg total RNA with a qScript cDNA synthesis kit (Quanta Biosciences) and by priming with random hexamers according to the manufacturer's instructions. Real-time quantitative PCR (RT-qPCR) was carried in a total volume of 10 μl with 1.5 μl of 1/10-diluted cDNA, 0.15 μM each primer specific for viral mRNA, and Fast Sybr green master mix (Applied Biosystems). The expression levels obtained for each gene with wild-type and vBcl-2-null mutant viruses were normalized to those of beta-actin. The fold change in expression for a particular gene of interest in response to lytic induction was subsequently calculated by comparing the level of expression to the normalized value for the wild-type virus at 24 h postinduction. The primers used were the following: for *orf50* (RTA), 5'-CACAAAATGGCGCAAGATGA-3' and 5'-TGGTAGAGTTGGGCCTTCAGTT-3'; for *orf59*, 5'-CGAGTCTTCGCAAAAGGTTTC-3' and 5'-AAGGGACCAACTGGTGTGAG-3'; for *orf65*, 5'-ATATGTGCGAGGC CGAATAC-3' and 5'-CCACCCATCCTCCTCAGATA-3'; for *orf16* (vBcl-2), 5'-ACCAGCTTGGGTTGAGCATG-3' and 5'-GGCTCGCCCC CAGTTC-3'; and for beta-actin, 5'-AATGTGGCCGAGGACTTTGATT GC-3' and 5'-AGGATGGCAAGGGACTTCTGTAA-3' (33). All PCRs were run in triplicate on a StepOne Plus real-time PCR system (Applied Biosystems Inc., Carlsbad, CA).

Purification and quantification of genomic DNA from infected cells. High-molecular-weight (HMW) DNA was extracted using a mammalian genomic DNA miniprep kit (Sigma). KSHV DNA was quantitated using a previously described TaqMan PCR employing primers and a probe targeting *orf K6* (39, 40). A second quantitative TaqMan-based real-time PCR assay detecting human endogenous RNase P (TaqMan human RNase P control kit; Applied Biosystems) was used as a normalization tool for HMW DNA and to confirm DNA quality. All PCRs were performed using a StepOne Plus real-time PCR system (Applied Biosystems Inc., Carlsbad, CA).

Antibodies and Western blot analysis. Cells were washed twice in cold phosphate-buffered saline (PBS), suspended in radioimmunoprecipitation assay lysis buffer, and incubated on ice for 30 min. Cell debris was removed by centrifugation at $12,000 \times g$ for 15 min at 4°C . Protein lysates were resolved by SDS-PAGE and transferred to nitrocellulose membranes using a Trans-Blot Turbo RTA midi-nitrocellulose transfer kit (Bio-Rad). The protein content of different samples was verified by Ponceau S staining. The nitrocellulose membranes were blocked with 5% dry milk in Tris-buffered saline and subsequently incubated with primary mouse antibodies to GFP (Covance Research Products), mCherry (catalog no. 632496; Clontech), tubulin (catalog no. E7-S; DSHB), beta-actin (catalog no. JLA20; Developmental Studies Hybridoma Bank [DSHB]) ORF45 (41), ORF K8 (42) (kindly obtained from Yan Yuan), ORF65 (43) (kindly obtained from Shou Jiang Gao), or RTA (44) (kindly provided by Keiji Ueda). Specific reactive bands were detected using antimouse antibody conjugated to horseradish peroxidase. Immunoreactive bands were visualized using an EZ enhanced chemiluminescence (ECL) detection kit (Biological Industries, Israel).

Quantification of infectious virus production. Various volumes of cell-free virus were used to infect SLK cells that were seeded at approximately 10^5 cells/well in 12-well plates 24 h prior to infection. The plates

were centrifuged at $1,500 \times g$ at 4°C for 60 min (spinoculation) in the presence of 8 $\mu\text{g/ml}$ Polybrene. Cells were collected 72 h later, washed twice with cold PBS, and suspended in 0.5 ml PBS; 0.5 ml 2% formaldehyde was added, and the cells were incubated at 4°C for 20 min. The cells were then washed with PBS, suspended in 1 ml 70% ethanol, and incubated for 30 min at 4°C . Finally, the cells were washed once and suspended in PBS. GFP-positive cells were determined using fluorescence-activated cell sorter (FACS) analysis (Gallios; Beckman Coulter). Data analysis was performed with FlowJo software. The titer for each inoculum size, assuming that one infectious particle generates a single GFP-positive cell, was calculated as a percentage of the number of uninfected cells, according to Poisson's law, and expressed as the number of infectious units per milliliter.

RESULTS

Construction of BAC16-vBcl-2-stop. To construct a virus that fails to express vBcl-2, we took advantage of the complete KSHV BAC16 clone, which enables genetic manipulation of the KSHV genome in *E. coli*. As previously described (36, 37) (see Materials and Methods), we used the BAC-based two-step bacteriophage lambda Red-mediated recombination system. Since *orf16* contains an in-frame methionine codon at position 18, which could potentially function as a translation initiation site, we selected this site as a target for the stop mutation. Therefore, this mutation was expected to abolish the expression of vBcl-2 and the potential expression of a shorter N-terminally truncated vBcl-2 as well. The final recombinant KSHV BAC16 containing a stop codon within *orf16*, designated BAC16-vBcl-2-stop, was tested for the presence of the engineered mutations by diagnostic PCR. To further confirm the mutation, we sequenced the genomic DNA, revealing one unintended nucleotide change (T \rightarrow C) at the third position of amino acid 17; however, this change did not change the amino acid sequence (Fig. 1A). Restriction enzyme analysis with BamHI revealed that BAC16 had a DNA fragmentation pattern similar to that of BAC16-vBcl-2-stop, and no rearrangements were detected. These analyses demonstrate that the vBcl-2 stop mutation was successfully inserted in the KSHV *orf16* gene.

Construction of a recombinant KSHV BAC16 expressing N-terminal mCherry-tagged vBcl-2. To construct a virus expressing the mCherry protein fused to the 5' end of vBcl-2, we generated a recombination cassette employing a universal mCherry transfer plasmid (see Materials and Methods). The resulting virus, BAC16-mCherry-vBcl-2, was expected to allow tracking of vBcl-2 during infection. The same cassette was also inserted into BAC16-vBcl-2-stop and was expected to express mCherry fused to the first 17 amino acids of vBcl-2 (BAC16-mCherry-vBcl-2-stop). Restriction enzyme analysis with BamHI indicated that BAC16-mCherry-vBcl-2 and BAC16-mCherry-vBcl-2-stop had similar DNA fragmentation patterns, with the exception of the 6,561-bp fragment predicted to undergo recombination. BAC16-mCherry-vBcl-2 and BAC16-mCherry-vBcl-2-stop contained the expected 7,269-bp restriction fragment. No additional differences were observed between the BAC16-mCherry-vBcl-2, BAC16-mCherry-vBcl-2-stop, and BAC16 viral DNAs following restriction enzyme digestion. To further confirm that faithful recombination had occurred, we PCR amplified and sequenced genomic DNA, including the boundaries of the targeting sequence used for allelic exchange. These experiments established that the recombinant genome contains the correct insertion with no evident rearrangements (Fig. 1B and C).

BAC16-mCherry-vBcl-2 exhibits functional properties similar to those of wild-type BAC16. To reconstitute infectious vi-

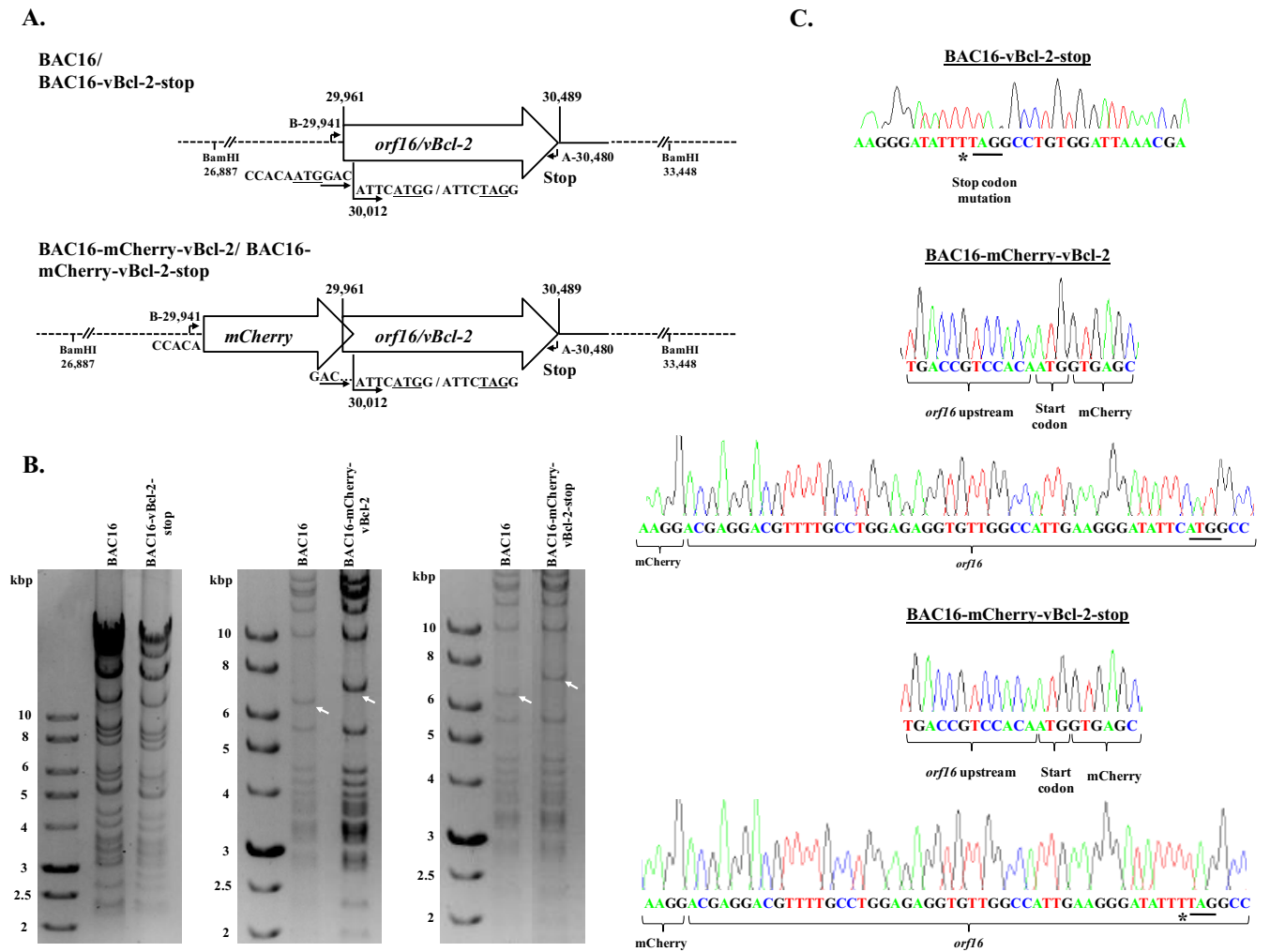


FIG 1 Construction and analysis of recombinant BAC16 containing a stop codon within *orf16* and expressing N-terminal mCherry-tagged vBcl-2. (A) Schematic illustration of the wild-type KSHV genome encoding *orf16/vBcl-2*. The indicated nucleotide positions refer to the sequence with GenBank accession number [GQ994935.1](https://www.ncbi.nlm.nih.gov/nuccore/GQ994935.1). The nucleotide positions of the vBcl-2 initiation methionine codon (ATG) and stop codon are indicated above the diagram. The second in-frame internal methionine codon is at position 30012 and is indicated below the diagram. The nucleotide sequences flanking the two potential initiation codons, as well as the stop mutation generated, are indicated below the diagram. Primers A and B, used to confirm the insertion and excision of the Kan^r/I-SceI cassette, are indicated. A schematic of the designed mCherry-tagged vBcl-2 (BAC16-mCherry-vBcl-2) and its corresponding mutant, vBcl-2-stop (BAC16-mCherry-vBcl-2-stop), is shown below the schematic for the wild-type BAC16 and mutated BAC16-vBcl-2-stop genomes. (B) Agarose gel electrophoresis of wild-type BAC16 and recombinant BAC16-vBcl-2-stop (left), recombinant BAC16-mCherry-vBcl-2 (middle), and BAC16-mCherry-vBcl-2-stop (right). DNAs were digested and resolved on a 0.4% agarose gel stained with ethidium bromide. Analysis of BAC16-vBcl-2-stop did not reveal any alteration in the restriction pattern. As predicted from the BamHI restriction pattern, the introduction of mCherry into BAC16 led to an increase in size from 6.5 to 7.3 kbp. Altered bands are indicated by white arrows. Molecular size markers are shown in the lanes on the left, and their sizes are indicated to the left of the gels. (C) Sequence analysis of wild-type BAC16 and the recombinant viruses with mutations at the stop site and at the mCherry-vBcl-2 junctions. An unintended nucleotide change is marked with an asterisk, while the ATG and stop codon mutation are underlined.

uses, HEK-293T cells were transfected with BAC16 and recombinant BAC16 DNAs, selected with hygromycin, and cocultivated with iSLK cells following TPA and sodium butyrate treatment. All further experiments employed iSLK cells, which permit efficient virus reactivation and virion production following doxycycline induction of RTA and sodium butyrate treatment (35, 45). To assess the level of replication of BAC16-mCherry-vBcl-2 in comparison to that of wild-type BAC16, we first induced the lytic cycle in infected iSLK cells. Proteins were extracted at 48, 72, and 96 h after induction and analyzed by Western blotting. As shown in Fig. 2, expression of mCherry-vBcl-2, detected with anti-mCherry antibody, was induced following lytic induction. As expected,

mCherry-vBcl-2 migrated at a molecular mass corresponding to ~48 kDa in cell extracts harboring BAC16-mCherry-vBcl-2. An additional band of ~37 kDa, which probably represents a cleavage product of mCherry, was also detected with the mCherry antibody. Further incubation of this blot with antibodies to the lytic gene products ORF45 and ORF65 and to GFP revealed the similar expression of these proteins following lytic induction, suggesting that the efficiency of lytic reactivation of BAC16-mCherry-vBcl-2 is similar to that of wild-type BAC16. Of note, previous studies by others (34) and by our group (data not shown) failed to identify the expression of vBcl-2 protein in cultivated cells, and to the best of our knowledge, the present study is the first to detect endoge-

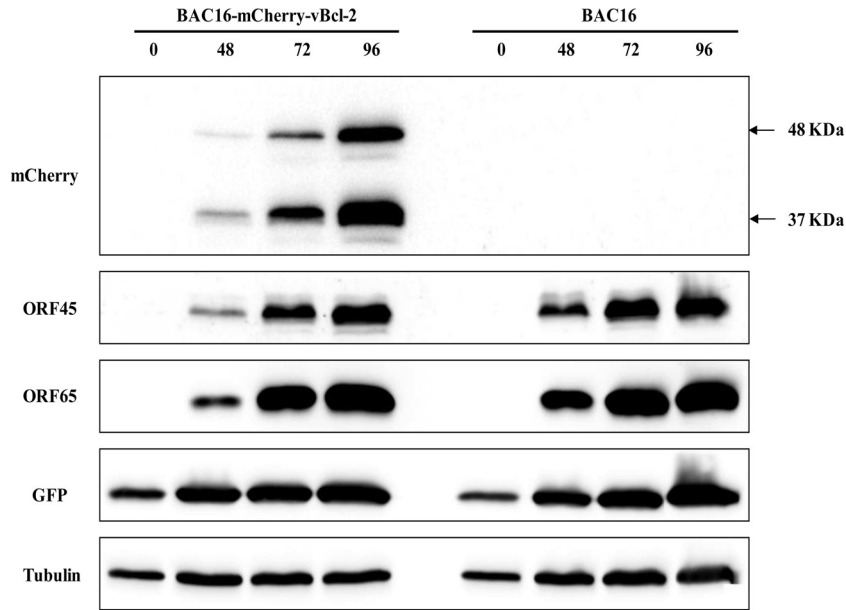


FIG 2 Comparison of the levels of KSHV gene expression in iSLK cells infected with BAC16 and BAC16-mCherry-vBcl-2. iSLK cells harboring BAC16 and BAC16-mCherry-vBcl-2 were induced to undergo lytic virus reactivation using sodium butyrate and doxycycline. At 0, 48, 72, and 96 h following induction, whole-cell lysates were prepared and protein expression by viral genes was analyzed by immunoblotting with the indicated antibodies against viral proteins, as well as GFP. The same blot was reprobbed with anti-tubulin as a loading control. Results from one experiment are shown and are representative of those from two experiments providing similar results.

nous vBcl-2 protein expression in KSHV-infected cell cultures. In this regard, Western blot analysis with anti-mCherry antibodies of lytically induced cells harboring BAC16-mCherry-vBcl-2 and cells infected with BAC16-mCherry-ORF45 revealed a large difference

in the expression level of the mCherry-tagged proteins, with mCherry-vBcl-2 being expressed at a lower level than mCherry-ORF45 (Fig. 3). Accordingly, we could not detect mCherry-vBcl-2 by immunofluorescence in the infected cells at different time

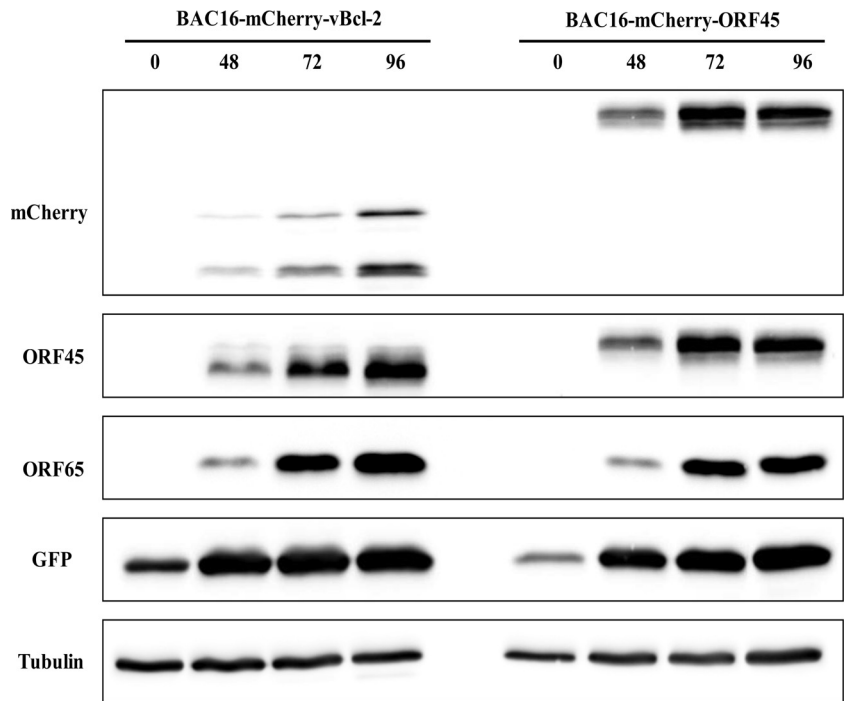


FIG 3 mCherry-vBcl-2 is expressed at relatively low levels compared to the levels of mCherry-ORF45 expression. iSLK cells harboring BAC16-mCherry-vBcl-2 and BAC16-mCherry-ORF45 were induced to undergo lytic virus reactivation and processed as described in the legend to Fig. 2. Results from one experiment are shown and are representative of those from three experiments providing similar results.

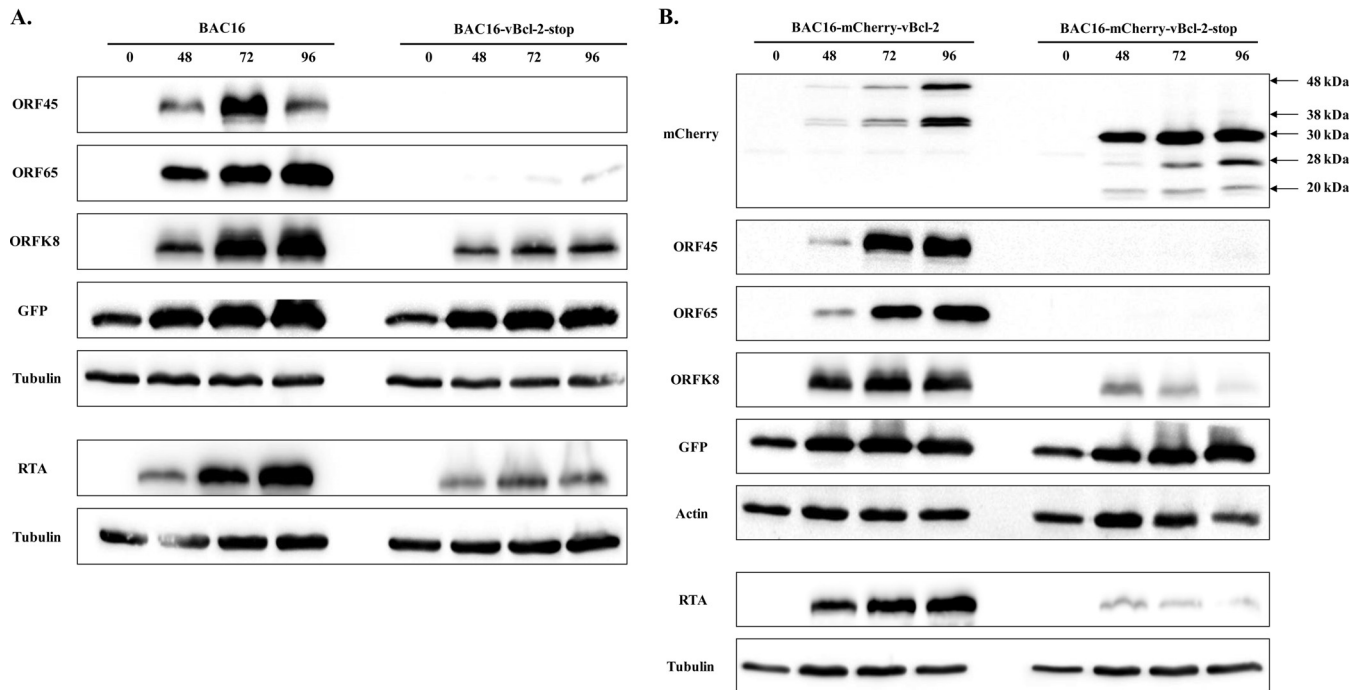


FIG 4 Comparison of the levels of KSHV gene expression in iSLK cells infected with wild-type and vBcl-2-stop mutants. iSLK cells harboring BAC16 versus BAC16-vBcl-2-stop (A) or BAC16-mCherry-vBcl-2 versus BAC16-mCherry-vBcl-2-stop (B) were induced to undergo lytic virus reactivation and processed as described in the legend to Fig. 2. Anti-beta-actin and anti-tubulin antibodies were used as loading controls. Results from one experiment are shown and are representative of those from three experiments providing similar results.

points following reactivation, probably due to its low levels of expression and the cleavage of mCherry.

Elimination of vBcl-2 expression strongly decreases lytic reactivation of KSHV. To investigate whether vBcl-2 is required for KSHV lytic reactivation, we explored the lytic cycle in cells infected with wild-type (BAC16 and BAC16-mCherry-vBcl-2) or mutant vBcl-2-null (BAC16-vBcl-2-stop and BAC16-mCherry-vBcl-2-stop) viruses. We induced the lytic cycle in infected iSLK cells, extracted proteins at 48, 72, and 96 h after induction, and analyzed protein expression by Western blotting. As shown in Fig. 4, lytic induction of wild-type virus-infected cells resulted in the accumulation of viral lytic proteins, including the immediate early gene product RTA, the early gene product K8, and the late protein ORF65. Accumulation of the ORF45 protein, which can be activated through RTA-dependent and -independent pathways (46), was evident as well. This was also associated with an increased expression of GFP, which was cloned in BAC16 and expressed under the constitutive EF-1 α cellular promoter (36). In contrast, lytic induction of cells infected with vBcl-2-null viruses was not associated with increased expression of viral lytic proteins, with the exception of the ORF K8 and RTA proteins, which were expressed at low levels. Notably, expression of RTA could result from the exogenous cassette, which is induced by doxycycline, and may not be due to induction of the viral lytic phase. In addition, similar levels of GFP expression were detected in cells infected with wild-type and vBcl-2-null viruses that were predominantly latent, suggesting that the lack of vBcl-2 does not affect the latent course. Finally, higher levels of expression of mCherry fused to the first 17 amino acids of vBcl-2 and de-

tected as a predominant ~30-kDa protein than mCherry-tagged vBcl-2 were noted, and these two proteins appeared to produce cleavage products, probably as a result of cleavage within the mCherry protein. Since the transcripts encoding mCherry and mCherry-vBcl-2 share the same promoter and translation initiation sites, the difference in the expression levels of these proteins is most likely posttranscriptionally controlled. Thus, inefficient translation of the vBcl-2 protein, inhibition of vBcl-2 translation, or a short protein half-life and a high rate of vBcl-2 degradation that prevents its accumulation could explain its low level.

By using real-time quantitative PCR (RT-qPCR), we measured the mRNA levels for *orf50* (RTA), *orf59*, and *orf65*, representing immediate early, early, and late viral genes, respectively, as well as the mRNA level for *orf16* (vBcl-2), prior to induction and at 24, 48, and 72 h postinduction (Fig. 5). Generally, the results were consistent with those of the protein analysis, though the increased sensitivity of the real-time PCR assay allowed documentation of small increases in the expression of the viral mRNAs in cells infected with vBcl-2-null viruses. As expected, the level of *orf16* mRNA was reduced in induced cells harboring vBcl-2-null viruses compared to that in induced cells harboring wild-type viruses. These results further suggest that the absence of vBcl-2 has a broad impact on viral gene expression following lytic reactivation.

Quantitative real-time PCR was performed to test for intracellular viral DNA replication and revealed a gradual increase in KSHV DNA levels following lytic induction of cells infected with either wild-type BAC16 (Fig. 6A) or BAC16-mCherry-vBcl-2 (Fig. 6B). At 72 h postinduction, this increase was ~5-fold lower in cells

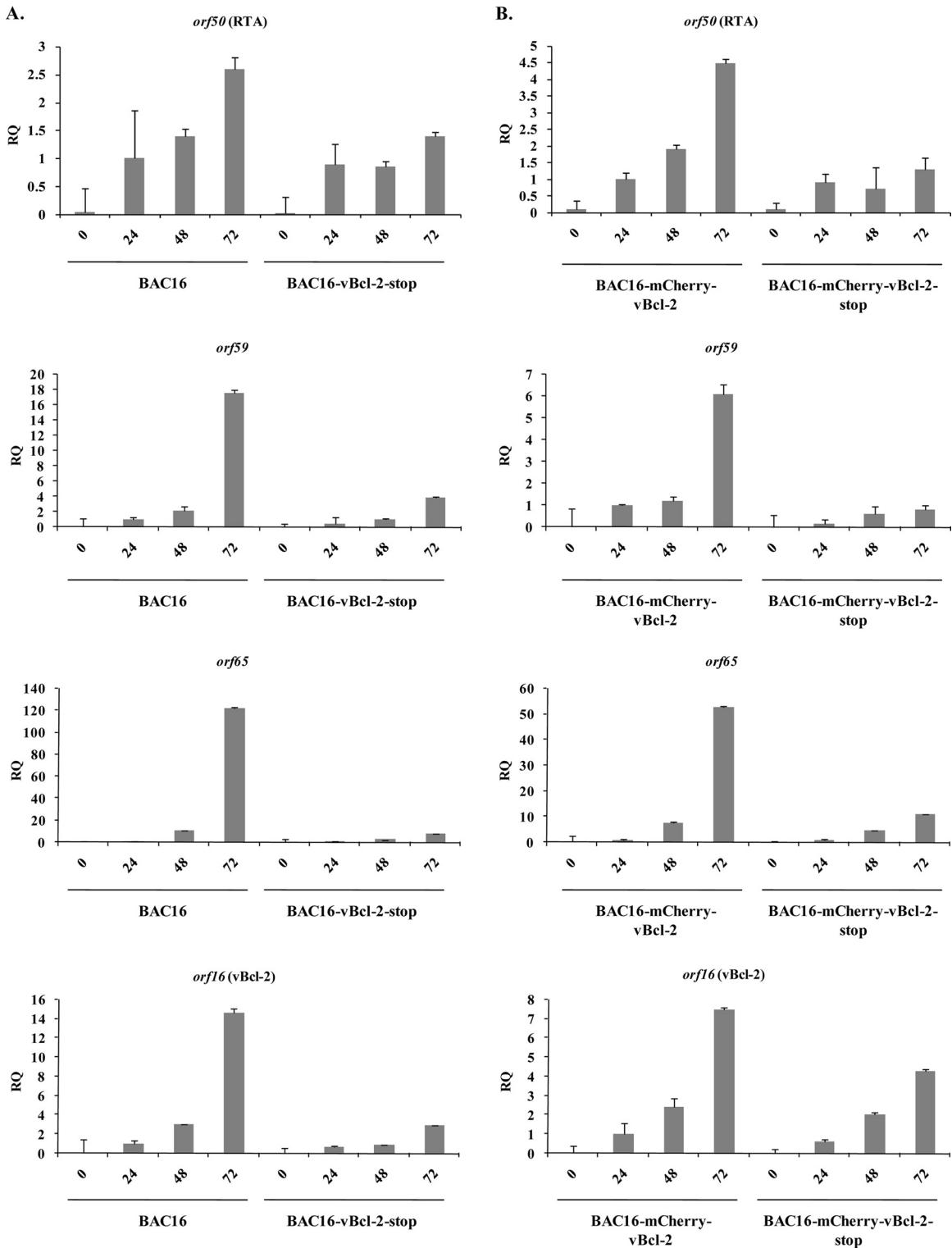


FIG 5 Quantification of effects of vBcl-2 on KSHV gene expression by RT-qPCR. RNA was isolated from iSLK cells that were infected with the indicated recombinant viruses (BAC16 and BAC16-vBcl-2-stop [A] or BAC16-mCherry-vBcl-2 and BAC16-mCherry-vBcl-2-stop [B]), and the abundance of specific viral mRNAs (*orf50* [RTA], *orf59*, *orf65*, *orf16*, and beta-actin) was measured by RT-qPCR. Analysis was performed with RNA harvested 24, 48, and 72 h after induction of lytic replication with doxycycline and sodium butyrate, while the corresponding untreated cells were used as controls. Each bar represents the average of the results from three repeats. The fold increase in mRNA abundance after induction relative to the amount of mRNA from wild-type virus at 24 h postinduction, which was defined as 1 after normalization to the amount of beta-actin, is shown. RQ, relative quantity. Results from one experiment are shown and are representative of those from three experiments providing similar results.

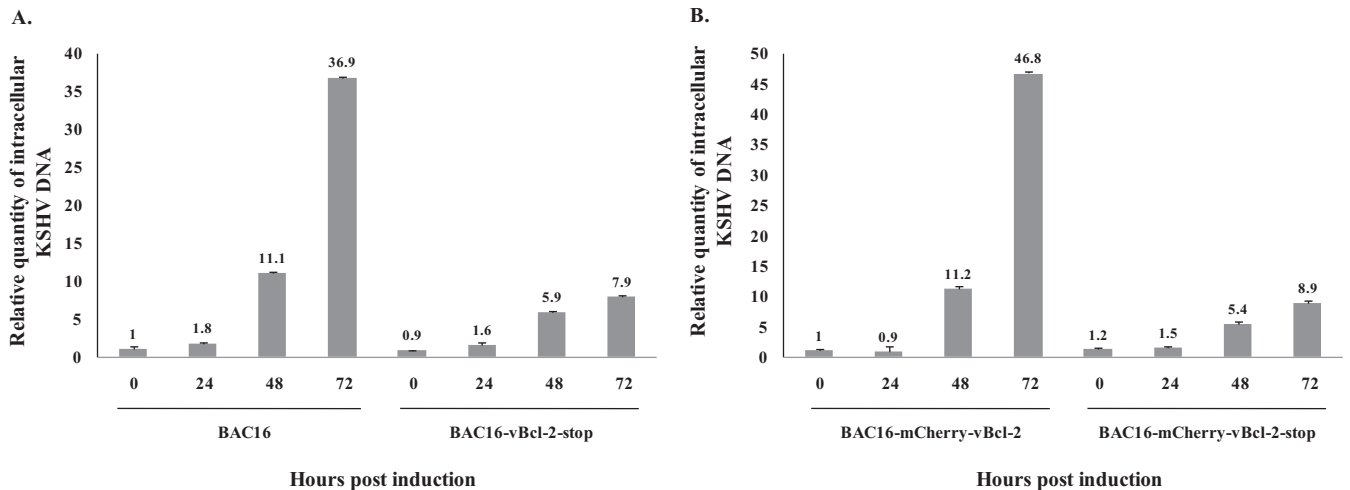


FIG 6 Comparison of the levels of KSHV DNA replication in iSLK cells infected with wild-type or vBcl-2 stop mutants. High-molecular-weight DNA was extracted at 0, 24, 48, and 72 h postinduction, and the number of KSHV genomes copies relative to the amount of cellular DNA was determined by quantitative TaqMan PCR. Values were normalized to the value for noninduced BAC16 (A) or BAC16-mCherry-vBcl-2 (B), which was defined as 1. The KSHV DNA level was normalized to the level of the human RNase P gene. Results from one experiment are shown and are representative of those from three experiments providing similar results.

infected with vBcl-2-stop (Fig. 6A) or mCherry-vBcl-2-stop (Fig. 6B) viruses than in those infected with wild-type virus, indicating impaired viral DNA replication in cells infected with vBcl-2-null viruses. Of note, latently infected cells that harbored wild-type and mutated viruses contained a similar number of copies of the KSHV genome, suggesting that vBcl-2 does not regulate the establishment or maintenance of KSHV latency in iSLK cells. Finally, we harvested extracellular virions from the supernatant of infected iSLK cells at 96 h postinduction and determined the number of infectious virions by FACS analysis of the percentage of GFP-positive cells. As shown in Fig. 7, the titers of the virus produced by cells infected with wild-type viruses reached 5×10^6 to 6×10^6 infectious units/ml, but the supernatants from iSLK cells

infected with vBcl-2-null viruses contained ~ 300 -fold lower numbers of infectious units.

DISCUSSION

Many viruses have evolved various strategies to prevent premature death of the host cell. Such strategies promote immune evasion, prolong survival of the infected cells, ensure increased virus propagation and dissemination, and may help viruses in the establishment and maintenance of persistent infections and tumorigenesis. The relative contributions and coordination of apoptotic and autophagy pathways during viral infection remain largely unknown. The two Bcl-2 homologs encoded by EBV are maximally expressed soon after infection but are neither expressed nor re-

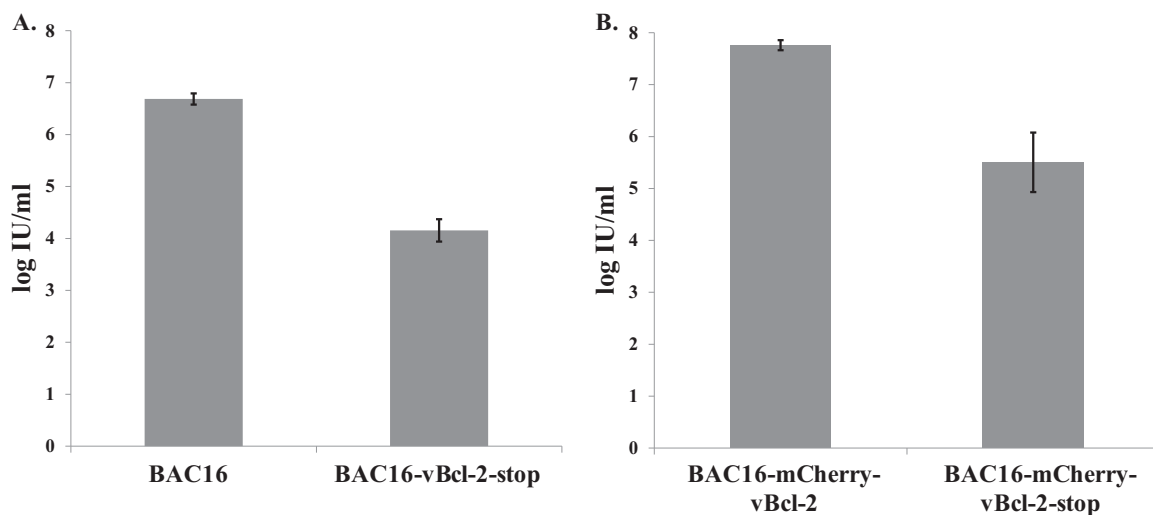


FIG 7 Reduced production of infectious virions by vBcl-2-stop recombinant viruses. Supernatants from iSLK cells infected with the different BAC16 recombinant viruses (BAC16 and BAC16-vBcl-2-stop [A] or BAC16-mCherry-vBcl-2 and BAC16-mCherry-vBcl-2-stop [B]) were collected at 96 h following lytic induction. Infectious virus titers were determined by FACS analysis of GFP-positive cells. Error bars represent standard deviations from 3 to 4 repeats. Results from one experiment are shown and are representative of those from three experiments providing similar results. IU, infectious units.

quired when latent infection is established (47). Mutant EBV lacking its two Bcl-2 homologs fails to transform primary resting B lymphocytes, and the infected cells die of immediate apoptosis, suggesting that these genes are essential for overcoming the initial apoptosis induced by viral infection (47). Studies with mutant murine gammaherpesvirus 68 (MHV-68) deficient for the Bcl-2 homolog M11 demonstrated no evidence of a contribution of M11 to lytic replication *in vitro*, but cells infected with this mutant virus did exhibit an impaired ability to establish latency and compromised reactivation from latency (22, 48–50). Further dissection of the role of the Bcl-2-mediated antiapoptotic versus antiautophagic functions of Bcl-2 during MHV-68 infection revealed that a mutant virus deficient in Beclin-1 binding, which is impaired in autophagy inhibition but retains intact antiapoptotic activity, is compromised in the maintenance of latency, though establishment of latency was unaffected. In contrast, infection with a Bcl-2 mutant virus defective in antiapoptotic activity was associated with a normal latent load but greatly impaired reactivation from latency (51). It therefore appears that Bcl-2 proteins function to delay apoptosis and autophagy, thereby supporting the establishment of latency and reactivation. Of note, M11 and vBcl-2 possess different relative affinities of binding to Beclin-1 and Bak, suggesting that viral Bcl-2 homologs may differ in their relative antiapoptotic versus antiautophagic activities (29).

In the present study, we demonstrate the expression of N-terminally tagged vBcl-2 in cultivated cells. In contrast to the levels of expression of mCherry-tagged ORF45 and of mCherry protein, which was expressed under the control of the same transcriptional control element as mCherry-vBcl-2, the level of vBcl-2 expression was low. This may account for the inability to detect the expression of vBcl-2 in KSHV-infected cell lines by using polyclonal antibodies produced by other groups (34) and in our lab (data not shown). This, together with the abundant cleavage of mCherry-vBcl-2, did not allow the use of immunofluorescence to track the expression of mCherry-vBcl-2 within cells. By using BAC16, a BAC clone harboring the full-length KSHV genome, we generated two vBcl-2-null recombinant viruses, BAC16-vBcl-2-stop and BAC16-mCherry-vBcl-2-stop, and examined their properties in comparison to those of their corresponding nonmutated viruses. The mutated viruses had comparable phenotypes. Both mutants could establish latent infection, suggesting that vBcl-2 is not necessary for the establishment of latent infection in iSLK cells. Yet unlike the wild-type virus, following lytic induction in cells containing the vBcl-2-null viruses, almost no lytic viral proteins were expressed, the increase in viral transcripts was largely impaired, viral DNA replication was reduced, and infectious virion production significantly decreased. These findings suggest that vBcl-2 is required for the expression of early and late lytic viral proteins and thereby affects DNA replication and the production of infectious virions. Thus, vBcl-2 appears to have an important role during the initial phases of reactivation and/or in sustaining the reactivation and promoting the subsequent cascade of the lytic phase. This effect could be indirectly mediated. Of note, our results indicate that although vBcl-2 is expressed at low levels, it has a critical role in the lytic phase. Given the known apoptosis and autophagy regulatory functions of vBcl-2 that involve its direct interaction with cellular proteins and thus require high levels of protein expression, it appears that vBcl-2 may have additional regulatory func-

tions beyond apoptosis and autophagy repression that do not depend on high levels of protein expression.

Of note, just before submission of the manuscript for this article, we found that our findings on the essential role of vBcl-2 during lytic reactivation were also obtained in an independent study conducted by Liang et al., the results of which are presented in the [accompanying paper](#) (52).

ACKNOWLEDGMENTS

We gratefully acknowledge Don Ganem, Rolf Renne, Nikolaus Osterrieder, Yan Yuan, Shou Jiang Gao, and Keiji Ueda for reagents and Thomas Schulz for his help with the implementation of the BAC system.

This work was supported by a grant from the Israel Science Foundation (grant no. 709/10).

REFERENCES

- Mesri EA, Cesarman E, Boshoff C. 2010. Kaposi's sarcoma and its associated herpesvirus. *Nat Rev Cancer* 10:707–719. <http://dx.doi.org/10.1038/nrc2888>.
- Kalt I, Masa SR, Sarid R. 2009. Linking the Kaposi's sarcoma-associated herpesvirus (KSHV/HHV-8) to human malignancies. *Methods Mol Biol* 471:387–407. http://dx.doi.org/10.1007/978-1-59745-416-2_19.
- Ganem D. 2010. KSHV and the pathogenesis of Kaposi sarcoma: listening to human biology and medicine. *J Clin Invest* 120:939–949. <http://dx.doi.org/10.1172/JCI40567>.
- Chang Y, Cesarman E, Pessin MS, Lee F, Culpepper J, Knowles DM, Moore PS. 1994. Identification of herpesvirus-like DNA sequences in AIDS-associated Kaposi's sarcoma. *Science* 266:1865–1869. <http://dx.doi.org/10.1126/science.7997879>.
- Cai Q, Verma SC, Lu J, Robertson ES. 2010. Molecular biology of Kaposi's sarcoma-associated herpesvirus and related oncogenesis. *Adv Virus Res* 78: 87–142. <http://dx.doi.org/10.1016/B978-0-12-385032-4.00003-3>.
- Gramolelli S, Schulz TF. 2015. The role of Kaposi Sarcoma-associated herpesvirus in the pathogenesis of Kaposi sarcoma. *J Pathol* 235:368–380. <http://dx.doi.org/10.1002/path.4441>.
- Dittmer DP, Damania B. 2013. Kaposi sarcoma associated herpesvirus pathogenesis (KSHV)—an update. *Curr Opin Virol* 3:238–244. <http://dx.doi.org/10.1016/j.coviro.2013.05.012>.
- Miller G, El-Guindy A, Countryman J, Ye J, Gradoville L. 2007. Lytic cycle switches of oncogenic human gammaherpesviruses. *Adv Cancer Res* 97:81–109. [http://dx.doi.org/10.1016/S0065-230X\(06\)97004-3](http://dx.doi.org/10.1016/S0065-230X(06)97004-3).
- Deng H, Liang Y, Sun R. 2007. Regulation of KSHV lytic gene expression. *Curr Top Microbiol Immunol* 312:157–183. http://dx.doi.org/10.1007/978-3-540-34344-8_6.
- Staudt MR, Dittmer DP. 2007. The Rta/Orf50 transactivator proteins of the gamma-herpesviridae. *Curr Top Microbiol Immunol* 312:71–100. http://dx.doi.org/10.1007/978-3-540-34344-8_3.
- Guito J, Lukac DM. 2012. KSHV Rta promoter specification and viral reactivation. *Front Microbiol* 3:30. <http://dx.doi.org/10.3389/fmicb.2012.00030>.
- Ye F, Lei X, Gao SJ. 2011. Mechanisms of Kaposi's sarcoma-associated herpesvirus latency and reactivation. *Adv Virol* 2011:193860. <http://dx.doi.org/10.1155/2011/193860>.
- Prasad A, Lu M, Lukac DM, Zeichner SL. 2012. An alternative Kaposi's sarcoma-associated herpesvirus replication program triggered by host cell apoptosis. *J Virol* 86:4404–4419. <http://dx.doi.org/10.1128/JVI.06617-11>.
- Gross A, McDonnell JM, Korsmeyer SJ. 1999. BCL-2 family members and the mitochondria in apoptosis. *Genes Dev* 13:1899–1911. <http://dx.doi.org/10.1101/gad.13.15.1899>.
- Walensky LD. 2006. BCL-2 in the crosshairs: tipping the balance of life and death. *Cell Death Differ* 13:1339–1350. <http://dx.doi.org/10.1038/sj.cdd.4401992>.
- Skommer J, Wlodkowic D, Deptala A. 2007. Larger than life: mitochondria and the Bcl-2 family. *Leuk Res* 31:277–286. <http://dx.doi.org/10.1016/j.leukres.2006.06.027>.
- Hardwick JM, Youle RJ. 2009. SnapShot: BCL-2 proteins. *Cell* 138:404. <http://dx.doi.org/10.1016/j.cell.2009.07.003>.
- Cuconati A, White E. 2002. Viral homologs of BCL-2: role of apoptosis in the regulation of virus infection. *Genes Dev* 16:2465–2478. <http://dx.doi.org/10.1101/gad.1012702>.

19. Cheng EH, Nicholas J, Bellows DS, Hayward GS, Guo HG, Reitz MS, Hardwick JM. 1997. A Bcl-2 homolog encoded by Kaposi sarcoma-associated virus, human herpesvirus 8, inhibits apoptosis but does not heterodimerize with Bax or Bak. *Proc Natl Acad Sci U S A* 94:690–694. <http://dx.doi.org/10.1073/pnas.94.2.690>.
20. Sarid R, Sato T, Bohenzky RA, Russo JJ, Chang Y. 1997. Kaposi's sarcoma-associated herpesvirus encodes a functional bcl-2 homologue. *Nat Med* 3:293–298. <http://dx.doi.org/10.1038/nm0397-293>.
21. Huang Q, Petros AM, Virgin HW, Fesik SW, Olejniczak ET. 2002. Solution structure of a Bcl-2 homolog from Kaposi sarcoma virus. *Proc Natl Acad Sci U S A* 99:3428–3433. <http://dx.doi.org/10.1073/pnas.062525799>.
22. Loh J, Huang Q, Petros AM, Nettesheim D, van Dyk LF, Labrada L, Speck SH, Levine B, Olejniczak ET, Virgin HW. 2005. A surface groove essential for viral Bcl-2 function during chronic infection in vivo. *PLoS Pathog* 1:e10. <http://dx.doi.org/10.1371/journal.ppat.0010010>.
23. Flanagan AM, Letai A. 2008. BH3 domains define selective inhibitory interactions with BHRF-1 and KSHV BCL-2. *Cell Death Differ* 15:580–588. <http://dx.doi.org/10.1038/sj.cdd.4402292>.
24. Chau BN, Cheng EH, Kerr DA, Hardwick JM. 2000. Aven, a novel inhibitor of caspase activation, binds Bcl-xL and Apaf-1. *Mol Cell* 6:31–40. [http://dx.doi.org/10.1016/S1097-2765\(05\)00021-3](http://dx.doi.org/10.1016/S1097-2765(05)00021-3).
25. Guo JY, Yamada A, Kajino T, Wu JQ, Tang W, Freel CD, Feng J, Chau BN, Wang MZ, Margolis SS, Yoo HY, Wang XF, Dunphy WG, Irusta PM, Hardwick JM, Kornbluth S. 2008. Aven-dependent activation of ATM following DNA damage. *Curr Biol* 18:933–942. <http://dx.doi.org/10.1016/j.cub.2008.05.045>.
26. Ojala PM, Yamamoto K, Castanos-Velez E, Biberfeld P, Korsmeyer SJ, Makela TP. 2000. The apoptotic v-cyclin-CDK6 complex phosphorylates and inactivates Bcl-2. *Nat Cell Biol* 2:819–825. <http://dx.doi.org/10.1038/35041064>.
27. Bellows DS, Chau BN, Lee P, Lazebnik Y, Burns WH, Hardwick JM. 2000. Antiapoptotic herpesvirus Bcl-2 homologs escape caspase-mediated conversion to proapoptotic proteins. *J Virol* 74:5024–5031. <http://dx.doi.org/10.1128/JVI.74.11.5024-5031.2000>.
28. Pattangre S, Tassa A, Qu X, Garuti R, Liang XH, Mizushima N, Packer M, Schneider MD, Levine B. 2005. Bcl-2 antiapoptotic proteins inhibit Beclin 1-dependent autophagy. *Cell* 122:927–939. <http://dx.doi.org/10.1016/j.cell.2005.07.002>.
29. Sinha S, Colbert CL, Becker N, Wei Y, Levine B. 2008. Molecular basis of the regulation of Beclin 1-dependent autophagy by the gamma-herpesvirus 68 Bcl-2 homolog M11. *Autophagy* 4:989–997. <http://dx.doi.org/10.4161/auto.6803>.
30. Liang C, Feng P, Ku B, Dotan I, Canaani D, Oh BH, Jung JU. 2006. Autophagic and tumour suppressor activity of a novel Beclin1-binding protein UVRAG. *Nat Cell Biol* 8:688–699. <http://dx.doi.org/10.1038/ncb1426>.
31. Wei Y, Pattangre S, Sinha S, Bassik M, Levine B. 2008. JNK1-mediated phosphorylation of Bcl-2 regulates starvation-induced autophagy. *Mol Cell* 30:678–688. <http://dx.doi.org/10.1016/j.molcel.2008.06.001>.
32. Paulose-Murphy M, Ha NK, Xiang C, Chen Y, Gillim L, Yarchoan R, Meltzer P, Bittner M, Trent J, Zeichner S. 2001. Transcription program of human herpesvirus 8 (Kaposi's sarcoma-associated herpesvirus). *J Virol* 75:4843–4853. <http://dx.doi.org/10.1128/JVI.75.10.4843-4853.2001>.
33. Yoo SM, Zhou FC, Ye FC, Pan HY, Gao SJ. 2005. Early and sustained expression of latent and host modulating genes in coordinated transcriptional program of KSHV productive primary infection of human primary endothelial cells. *Virology* 343:47–64. <http://dx.doi.org/10.1016/j.virol.2005.08.018>.
34. Widmer I, Wernli M, Bachmann F, Gudat F, Cathomas G, Erb P. 2002. Differential expression of viral Bcl-2 encoded by Kaposi's sarcoma-associated herpesvirus and human Bcl-2 in primary effusion lymphoma cells and Kaposi's sarcoma lesions. *J Virol* 76:2551–2556. <http://dx.doi.org/10.1128/jvi.76.5.2551-2556.2002>.
35. Myoung J, Ganem D. 2011. Generation of a doxycycline-inducible KSHV producer cell line of endothelial origin: maintenance of tight latency with efficient reactivation upon induction. *J Virol Methods* 174:12–21. <http://dx.doi.org/10.1016/j.jviromet.2011.03.012>.
36. Brulois KF, Chang H, Lee AS, Ensser A, Wong LY, Toth Z, Lee SH, Lee HR, Myoung J, Ganem D, Oh TK, Kim JF, Gao SJ, Jung JU. 2012. Construction and manipulation of a new Kaposi's sarcoma-associated herpesvirus bacterial artificial chromosome clone. *J Virol* 86:9708–9720. <http://dx.doi.org/10.1128/JVI.01019-12>.
37. Tischer BK, von Einem J, Kaufer B, Osterrieder N. 2006. Two-step Red-mediated recombination for versatile high-efficiency markerless DNA manipulation in *Escherichia coli*. *Biotechniques* 40:191–197. <http://dx.doi.org/10.2144/000112096>.
38. Bergson S, Kalt I, Itzhak I, Brulois KF, Jung JU, Sarid R. 2014. Fluorescent tagging and cellular distribution of the Kaposi's sarcoma-associated herpesvirus ORF45 tegument protein. *J Virol* 88:12839–12852. <http://dx.doi.org/10.1128/JVI.01091-14>.
39. Guttman-Yassky E, Abada R, Kra-Oz Z, Sattinger J, Perelman A, Bergman R, Sarid R. 2007. Relationship between human herpesvirus 8 loads and disease stage in classic Kaposi sarcoma patients. *Diagn Microbiol Infect Dis* 57:387–392. <http://dx.doi.org/10.1016/j.diagmicrobio.2006.09.012>.
40. de Sanjose S, Marshall V, Sola J, Palacio V, Almirall R, Goedert JJ, Bosch FX, Whitby D. 2002. Prevalence of Kaposi's sarcoma-associated herpesvirus infection in sex workers and women from the general population in Spain. *Int J Cancer* 98:155–158. <http://dx.doi.org/10.1002/ijc.10190>.
41. Zhu FX, Chong JM, Wu L, Yuan Y. 2005. Virion proteins of Kaposi's sarcoma-associated herpesvirus. *J Virol* 79:800–811. <http://dx.doi.org/10.1128/JVI.79.2.800-811.2005>.
42. Wang Y, Li H, Tang Q, Maul GG, Yuan Y. 2008. Kaposi's sarcoma-associated herpesvirus ori-Lyt-dependent DNA replication: involvement of host cellular factors. *J Virol* 82:2867–2882. <http://dx.doi.org/10.1128/JVI.01319-07>.
43. Ye F, Zhou F, Bedolla RG, Jones T, Lei X, Kang T, Guadalupe M, Gao SJ. 2011. Reactive oxygen species hydrogen peroxide mediates Kaposi's sarcoma-associated herpesvirus reactivation from latency. *PLoS Pathog* 7:e1002054. <http://dx.doi.org/10.1371/journal.ppat.1002054>.
44. Ueda K, Ishikawa K, Nishimura K, Sakakibara S, Do E, Yamaniishi K. 2002. Kaposi's sarcoma-associated herpesvirus (human herpesvirus 8) replication and transcription factor activates the K9 (vIRF) gene through two distinct cis elements by a non-DNA-binding mechanism. *J Virol* 76:12044–12054. <http://dx.doi.org/10.1128/JVI.76.23.12044-12054.2002>.
45. Sturzl M, Gaus D, Dirks WG, Ganem D, Jochmann R. 2013. Kaposi's sarcoma-derived cell line SLK is not of endothelial origin, but is a contaminant from a known renal carcinoma cell line. *Int J Cancer* 132:1954–1958. <http://dx.doi.org/10.1002/ijc.27849>.
46. Chang PJ, Wang SS, Chen LY, Hung CH, Huang HY, Shih YJ, Yen JB, Liou JY, Chen LW. 2013. ORF50-dependent and ORF50-independent activation of the ORF45 gene of Kaposi's sarcoma-associated herpesvirus. *Virology* 442:38–50. <http://dx.doi.org/10.1016/j.virol.2013.03.023>.
47. Altmann M, Hammerschmidt W. 2005. Epstein-Barr virus provides a new paradigm: a requirement for the immediate inhibition of apoptosis. *PLoS Biol* 3:e404. <http://dx.doi.org/10.1371/journal.pbio.0030404>.
48. de Lima BD, May JS, Marques S, Simas JP, Stevenson PG. 2005. Murine gammaherpesvirus 68 bcl-2 homologue contributes to latency establishment in vivo. *J Gen Virol* 86:31–40. <http://dx.doi.org/10.1099/vir.0.80480-0>.
49. Gangappa S, van Dyk LF, Jewett TJ, Speck SH, Virgin HW. 2002. Identification of the in vivo role of a viral bcl-2. *J Exp Med* 195:931–940. <http://dx.doi.org/10.1084/jem.20011825>.
50. Herskowitz J, Jacoby MA, Speck SH. 2005. The murine gammaherpesvirus 68 M2 gene is required for efficient reactivation from latently infected B cells. *J Virol* 79:2261–2273. <http://dx.doi.org/10.1128/JVI.79.4.2261-2273.2005>.
51. E X, Hwang S, Oh S, Lee JS, Jeong JH, Gwack Y, Kowalik TF, Sun R, Jung JU, Liang C. 2009. Viral Bcl-2-mediated evasion of autophagy aids chronic infection of gammaherpesvirus 68. *PLoS Pathog* 5:e1000609. <http://dx.doi.org/10.1371/journal.ppat.1000609>.
52. Liang Q, Chang B, Lee P, Brulois KF, Ge J, Shi M, Rodgers MA, Feng P, Oh B-H, Liang C, Jung JU. 2015. Identification of the essential role of viral Bcl-2 for Kaposi's sarcoma-associated herpesvirus lytic replication. *J Virol* 89:5308–5317. <http://dx.doi.org/10.1128/JVI.00102-15>.